Increased airborne transmission of COVID-19 with new variants.

Implications for health policies.

Bertrand.R. Rowe[a], André Canosa[b], Amina Meslem[c] and Frantz Rowe[d,e]

[a]*Rowe Consulting, 22 chemin des moines, 22750 Saint Jacut de la Mer (France).*

bertrand.rowe@gmail.com

[b]*CNRS, IPR (Institut de Physique de Rennes)-UMR 6251, Université de Rennes, 35000 Rennes, (France).*

andre.canosa@univ-rennes1.fr

[c]*Université de Rennes, LGCGM, 3 Rue du Clos Courtel, BP 90422, 35704, Rennes, CEDEX 7, (France).*

amina.meslem@univ-rennes1.fr

[d]*Nantes Université, LEMNA, Nantes, (France).*

[e]*SKEMA Business School, KTO, Sophia-Antipolis, France (France).*

frantz.rowe@univ-nantes.fr

Supplementary materials

SM1- Host entry characteristics:

As discussed in the main paper the quantum of contagium, as defined by Wells [1], considers a variety of mechanisms including pathogen inhibition by host defenses. These defenses include, beside microbiological phenomena (immune response and others), some physical processes described below that are important for contamination by the aerosol route.

In a series of remarkable experiments with rabbits and mice, Wells demonstrated that, concerning aerosols, very fine particles (which include dry nuclei) have a much higher infectious power than coarse particle, at least for disease such as tuberculosis and influenza. Wells' explanation was that the human body has a very efficient system to prevent coarse particle larger than a few micrometers to penetrate deep in the respiratory system. Beside defenses against very coarse particles, specific to the upper respiratory tract (nostrils, nasal cavity, mouth, throat, pharynx), and voice box (larynx)), mucociliary clearance is a primary innate defense mechanism of the lung (see the reviews by Bustamante-Marin and Ostrowski [2] and Kuek [3]) that helps to remove smaller particles and pathogens from the lower respiratory tract, using the epithelium formed by ciliated and secretory cells. These later provide a mucus which is expelled by cilia toward the digestive system after swallowing. It is known that most respirable pathogens do not provoke illness when ingested, and there is currently no evidence that COVID-19 could be transmitted by ingestion [4]. Note that the mechanism of very fine particles deposition into the lungs has been the subject of numerous studies for mineral toxic dusts, such as asbestos [5].

Nowadays, the formidable progress of microbiology allows studying the influence of cellular characteristics on the vulnerability of cells to coronaviruses, which start with binding of the viral spike (S) proteins to cellular receptors [6]. Following some data, it has been anticipated that infectivity was higher in the upper respiratory tract and that the nose was a primary target [7]. However the severity of the COVID-19 is linked to the occurrence of pneumonia, followed by acute diffuse alveolar damage, which can be due to direct lung infection by airborne microparticles [8,9] or by indirect infection from the oropharynx to the lung by aspiration of the viral inoculum when breathing [7]. Also the study of nonhuman primate model reveals, after autopsy, the importance of lung lesions in macaques [10]. It seems reasonable to assume that, when the virus reaches the lungs directly, before some immunity able to inhibit viral reproduction has been acquired, it could result in devastating pneumonia, as sometimes reported in young, healthy subjects.

It has to be noticed that as well the remarkable experimental results of Wells for particle size than the most recent findings of microbiology cannot be directly used to develop a quantitative model of transmission risk. Therefore, some concepts and approaches must be developed prior to the establishment of any risk model.

SM2- Conservation and transport equations

It is far beyond the possibility of this section of the supplementary materials to develop the complexity of transport and conservation equations for diphasic turbulent fluids, with the target of precise calculations of the fields of velocities, temperature and concentrations of the various components. We shall just present the equation used in the main paper for the case of a well-mixed room (homogeneous hypothesis) and the approach underlying much of the calculations used in inhomogeneous models in order to calculate the concentration field of infectious particles.

In a homogeneous model, it is assumed that there is no spatial gradient of risk in a space where the infectors and the receivers either evolve or stay in place. In other words, it is assumed that the infectious microdroplets are evenly distributed. This is typical of two kinds of situations. It happens first instantly in a space where high performance mixing ventilation is achieved using special air terminal units designed to promote a high jet induction (i.e., vortex diffusers, lobed diffusers). This case lies to forced convection state. In absence of this kind of mixing ventilation there are a variety of air motions induced by other phenomena, such as natural convection, wake of moving people, door openings for letting people in or out. It can be shown that in many situations of this sort, the well mixed room hypothesis is also valid [11]. Then, we consider an evenly distribution of microdroplets obtained by induced turbulent flows, although this distribution is not really continuous due to its discrete character (very low concentration). Using CO_2 as a proxy of infectious microdroplets (i.e. quanta), observations show that this condition is most often fulfilled (see main paper).

Of course, if specific ventilation techniques are used [12], the generated directional air flows within the room lead to preferential aerosols trajectories following air distribution patterns.

In a homogeneous model it is possible to write a conservation equation for the concentration n_i of mono-sized microdroplets in a volume V, as developed by Rowe et al [13] for the indoor risk assessment, to compare with the outdoor case. Figure SM2-1 depicts the situation:

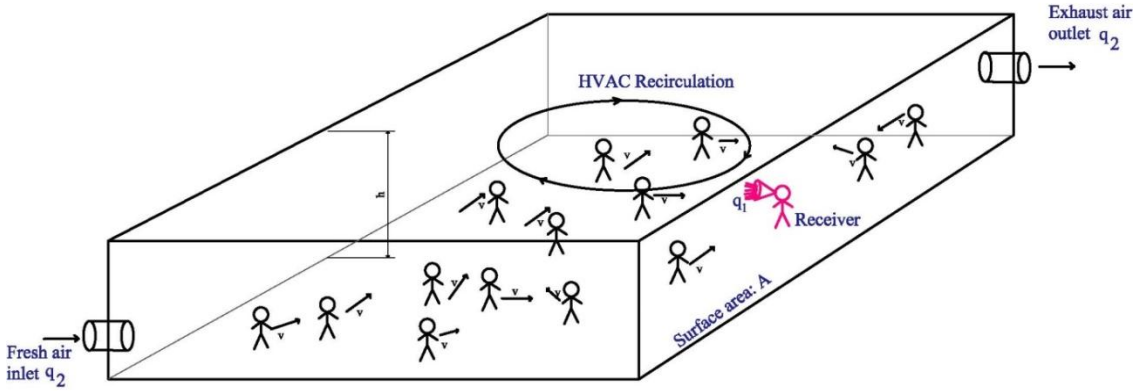

Figure SM2-1: a typical indoor homogeneous situation.

In this figure the inlet and outlet ventilation flow rates are assumed equal with the value q_2. Let N_p be the number of people inside, $N_i(t)$ the total number of aerosol particles of human respiratory origin inside the volume, resulting in a concentration of particles of $n_i(t) = N_i(t)/V$. The mean exhaled flow rate of a person was taken as p (of course identical to the inhaled rate) and the concentration of particles in this flow was assumed equal to n_1

(SM2-1) $$\frac{dN_i}{dt} = V \times \frac{dn_i}{dt} = N_p \times p \times n_1 - q_2 \times n_i$$

It was assumed no sink term for the particles inside the volume.

In the same way, an equation of conservation can be applied to the quanta of contagium as defined by Wells [1]. Let N_q be the total number of quanta in the volume V and n_q the quantum concentration. Considering the quantum production rate per infector q and introducing a quantum lifetime, which can be considered as the virus lifetime, τ_i , this equation reads:

(SM2-2) $$\frac{dN_q}{dt} = V \times \frac{dn_q}{dt} = I \times q - q_2 \times n_q - \frac{n_q}{\tau_i} \times V$$

In this equation we consider the number of infectors I within the volume since only infectors emit quanta.

Assuming $n_q(0) = 0$, The solution of (SM2-2) is:

(SM2-3) $$n_q(t) = n_q^{\infty} \times \left[1 - exp\left(-\frac{t}{\tau_1}\right)\right]$$

with:

(SM2-4) $$\tau_1 = \frac{V}{q_2 + \frac{V}{\tau_i}}$$

The concentration of quanta at stationary state i.e. $t \sim a\ few\ \tau_1$ is:

(SM2-5) $$n_q^{\infty} = \frac{I \times q}{(q_2 + \frac{V}{\tau_i})}$$

which, if the virus lifetime is neglected, reduces to:

(SM2-6) $$n_q^{\infty} = \frac{I \times q}{q_2}$$

Note that if a device able to sterilize a flow rate q_3 is used, the above equations hold just by replacing q_2 by $Q = q_2 + q_3$.

These equations funded on the well mixed room hypothesis are the basis of the famous Wells-Riley model and are convenient for a very large number of indoor situations. However, inhomogeneous infection patterns are reported for a number of well-documented transmission events in closed spaces, especially in restaurants [14-16] but also in other places such as aircrafts [17]. Generally, in these specific well studied cases, inhomogeneity was created by the mechanical ventilation system of air conditioning (hereafter AC) with recirculation, inducing locally larger air velocity. One typical and largely mediatized event concerned a restaurant in Guangzhou, China. It has been the subject of numerical modeling [14]. Numerous published works in the field do not relate to a specific observed event but to hypothetical situations supposed to represent typical cases, such as a supermarket [18]. These models rely on CFD (Computational Fluid Dynamics) calculations of the air flow stream, using a variety of software, such as Open Foam for example. Then the microparticle behavior is estimated using a variety of methods (Lagrangian, Monte-Carlo). In the Lagrangian approach the movement of each particle is calculated using Newton's second law of motion, where, within forces acting on the particle, the drag one is determined from the calculated field of air velocity. Note that, for a Stokes number << 1, the particles are just assumed to follow the flow. The Stokes number can be defined as the ratio of two times τ_a/τ_h , τ_a being the time of velocity accommodation of a particle to the flow velocity and τ_h the hydrodynamic time (equal to a typical length of the problem divided by the flow velocity). The Stokes number reads [19]:

$$St = \frac{D_p^2 \times \rho_p \times C_c \times u_0}{18 \times \mu \times L}$$

With D_p and ρ_p being respectively the diameter and volume mass of the particle, μ the air viscosity, u_0 and L respectively a typical order of magnitude of flow velocity and length. C_c is a slip parameter which takes into account the value of the particle Knudsen number. For particles of the size considered in airborne transmission C_c is very close to one. Note that L/u_0 is the hydrodynamic time and that for most problems dealing with the behavior of exhaled aerosol particles in indoor situation the Stokes number remains much smaller than one, except for large particles in the close contact case discussed in next section.

Il is also worthwhile to point out that when inhomogeneous infection modeling is applied to a specific geometry of the environment, it can be applied as such for the design of a new building for example but is limited for applications in the real life of most existing buildings and therefore, on the short term, for driving public policy. What is more interesting is the modeling of airborne close contact discussed in the next section.

SM3- Close contact transmissions

It is now largely admitted that the transmission of COVID-19 disease by close contact is most often an airborne one, referred in the literature as “short-range airborne transmission” [20,20,21,21]. Close to the emitter the turbulent expiratory plume (or puff for cough and sneeze) can have a much higher quantum (viral) load than in the ambient air of the indoor space considered. Several models of this phenomena have been proposed, some very simple [20] others more sophisticated. The recent one by Cortellessa *et al.* [21] employs CFD for the air flow and Lagrangian calculations for the particles to derive the dose and the risk as a function of the distance between infector and susceptible. Not only the distance but also the time of exposure is considered in order to assess the risk, although the time is limited to fifteen minutes. Large microdroplets which behave in a ballistic way are also considered and shown to prevail only at very short distance (< 60 cm), with a contribution to the dose being completely negligible at higher distances, demonstrating the airborne character of most airborne contamination in close contact, excepted intimate.

In their paper, Cortellessa *et al*. also made a comparison with the homogeneous risk. However, the comparison is restricted to the same time of exposure of fifteen minutes, with an initial concentration of quanta equal to zero. Therefore, it does not consider long times of exposure for the homogeneous case at steady state, as found for example in schools but such an extension can easily be done. Indeed, a good comparison should have to include the probability of close contacts together with contact durations, which is not done. Such a close contact risk assessment is anyway extremely useful for public policy.

SM4- Infector proportion and combination analysis

The problem of determining the exact proportion r of infectors I in a large population N_{Tot} ($r = I/N_{Tot}$) is a difficult one. Two statistical results are most often available. The positivity rate is the number of populations tested positive related to the total number of people tested, and therefore is a proportion without dimension. The incidence rate is the number of new people tested positive in a population, which can then be reported to a target population (for example 10^5 individuals) for a given period of time (for example one day or one week). It is therefore a temporal rate and, as such, has the dimension of (time)$^{-1}$. It is clear from these definitions that the results will depend on which people are tested and also of the size of the target. Since many people are infected but not tested and that people tested positive in the past remain infectious for some time, it can be anticipated that the real number of infectors could be much higher than what can be deduced from an analysis of the incidence rate: in principle, this rate can drop to zero with still infectors in the population. Further, since the population tested is often a symptomatic one, the positivity rate of testing could be much higher than the real proportion of infectors. Only a blind testing of a representative population would lead a true value of r.

Therefore the purpose of the present SM is just to show that it is possible to estimate the probability of infection of a susceptible target using a simplified expression (see SM4-3) which essentially considers the given proportion of infectors *r* in a population of N_{Tot} individuals, provided that the ventilation flow rate per person, q_{norm}, is known and the time of exposure *t* is fixed. Here N_{Tot} will represent the inhabitants of a country, a region, a metropole or a city or it can also denote a fixed reference population like 100000, for instance. Then, N_{Tot} is large. The number of infected people in that population will be quoted I further in the text (see SM4-6 and beyond) with $I = r \times N_{Tot}$.

In the main paper we have derived an equation for the dose inhaled by a susceptible person:

(SM4-1) $$X = \frac{r \times p}{q_{norm}} \times q \times t$$

which assumes that the total ventilation rate q_2 is given by $q_{norm} \times N_p$, where N_p is the number of people present, with the susceptible target, in a specific location. Here $N_p \ll N_{Tot}$. It is also assumed that the proportion of infected people r is also representative of the sanitary situation in the space of interest. In other words, if n is the number of infectors in the restricted population of N_p persons, we assume that $r = n/N_p = I/N_{Tot}$. We also remember that p and q are the respiratory flow rate and the quantum rate of pathogens per infector expressed in h^{-1}, respectively.

From this, the probability of infection is given by the Wells-Riley expression already presented in the main text (eq. 3):

(SM4-2) $$P_{WR} = 1 - exp(-X)$$

or

(SM4-3) $$P_{WR} = 1 - exp^{\left(-\frac{r\,p}{q_{norm}} qt\right)}$$

Another way to calculate this probability, which seems to be more realistic, is to make a weighted summation of probabilities to be infected in conditions where one, two, three etc. infectors are present in the restricted population of N_p people. This can be expressed as:

(SM4-4) $$P = \sum_1^{N_p} P_n(r) \times P_{WR}(n)$$

where $P_n(r)$ is the probability to have n infectors and $P_{WR}(n)$ the Wells Riley probability of being infected with n infectors in the population of N_p individuals. Then:

(SM4-5) $$P_{WR}(n) = 1 - exp^{-\frac{n\,p}{q_2}qt}$$

This new expression SM4-4 has an interesting advantage with respect to the simpler equation SM4-3 since it discriminates the individual $P_n(r)$ contributions from each other. Then, it is possible to evaluate how significant is each term in the summation and more particularly if the state with only one infector can be representative of the total risk of infection or not.

Probability $P_n(r)$ is dependent on the number of infected people I and consequently it is also a function of r. It can be derived from a combinatory analysis. Defining $C_{N_{Tot}}^{N_p}$ as the number of combinations of selecting an ensemble of N_p persons in a larger group of N_{Tot} individuals, one can express the number of combinations that include n individuals with a given property (here infection) in the selected group of N_p people. Then the probability of having n individuals infected in the restricted population N_p is simply given by:

(SM4-6) $$P_n(r) = \frac{C_I^n\, C_{N_{Tot}-I}^{N_p-n}}{C_{N_{Tot}}^{N_p}}$$

We remember here that the number of combinations of i elements in a global ensemble of j objects (with j ≥i) is mathematically equal to:

(SM4-7) $$C_j^i = \frac{(j)!}{(i)!(j-i)!}$$

From this, equation SM4-4 becomes:

(SM4-8) $$P = \sum_1^{N_p} \frac{C_I^n\, C_{N_{Tot}-I}^{N_p-n}}{C_{N_{Tot}}^{N_p}} \times \left(1 - exp^{-\frac{n\,p}{q_2}qt}\right)$$

This expression is numerically evaluated below for a few examples and compared to equation SM4-3. We consider here situations for which the restricted population is smaller than the total number of infectors in the reference population N_{Tot}:

(SM4-9) $$N_p < I$$

Calculations are be made considering a reference population N_{Tot} of 10^5; a respiratory flow rate p of 0.5 m^3/h; a quantum infection rate q of 40 h^{-1} and a time of exposure t of 2 hours. A standard ventilation flow rate q_{norm} of 20 m^3/h/person will be also employed. The proportion of infected people r is varied between 0.001 and 0.03 and the restricted population N_p is chosen as either 80 or 30. From this, the number of infected people in the N_{Tot} main group will vary from 100 to 3000 according to the r value, thus respecting inequality SM4-9.

Results of SM4-3 and SM4-8 are presented in Table SM4-1 and SM4-2 for the two values of N_p. In addition, we indicate the limit of n, quoted n_{cut}, beyond which $P_n(r) \times P_{WR}(n)$ terms do not contribute significantly to the summation in SM4-8; the value of n, quoted n_{max}, corresponding to the main contribution $P_{n_{max}}(r) \times P_{WR}(n_{max})$ in the summation and the percentage of this contribution to P value.

Table SM4-1: Comparison of P_{WR} with P for a restricted population N_p of 80 individuals

r	P_{WR} (SM4-3) %	P (SM4-8) %	n_{cut}	n_{max}	n_{max} contribution %
0.001	0.200	0.197	2	1	93
0.003	0.598	0.591	3	1	79
0.010	1.980	1.956	4	1	46
0.030	5.824	5.756	8	3	27

Table SM4-2: Comparison of P_{WR} with P for a restricted population N_p of 30 individuals

r	P_{WR} (SM4-3) %	P (SM4-8) %	n_{cut}	n_{max}	n_{max} contribution %
0.001	0.200	0.193	2	1	97
0.003	0.598	0.579	2	1	92
0.010	1.980	1.917	3	1	75
0.030	5.824	5.644	5	1	43

These calculations demonstrate a very good agreement between both ways of determining the probability of infection from either P_{WR} or P. The agreement is even better when the restricted population is enhanced, essentially due to the statistical effect of using larger N_p numbers. It can also be shown that the contribution of one infector (n_{max}=1) in the summation is the main one in many situations although, however, summation cannot be limited to the first term in SM4-8 for several conditions as indicated by the n_{cut} value and the "n_{max} contribution" columns. The lower the proportion of infectors r, the larger the contribution of $P_1(r) \times P_{WR}(1)$ which makes a lot of sense since for small r the probability of having more than one infector in the restricted population N_p becomes very small.

To conclude we stress that we have restricted the demonstration to a limited number of configurations but it is worth pointing out that several parameters act in a similar way mathematically speaking. Then, changing the time of exposure or/and the quantum rate of infectors would lead to essentially the same kind of conclusions.

SM5- Masks, quantum production rate and inhaled dose

To build a probabilistic model of infection it is necessary to know the production rate of quanta (as defined by Wells) by an infector. It is defined per unit time and per infector (unit: h^{-1} for example) and can be deduced from epidemiological observations [22] but also linked to the distributions of microdroplets emitted by humans, together with the knowledge of viral load in respiratory fluids and of the mean number of viruses required to infect 63% of susceptibles.

As stated in the main paper and following Buonanno *et al.* [23], the quantum production rate q can be written as:

(SM5-1) $$q = VL \times c \times p \times \int_0^{10\mu m} N_d(D) \times dV_d\,(D)$$

where VL is the viral load in the respiratory fluid, c is a factor of proportionality between the viral content (copies/unit volume) and quanta, p is the pulmonary exhaled volume rate (volume/unit time), $N_d(D)$ the size distribution of droplets (diameter D) of volume V_d.

Morawska *et al*. [24] have shown that microdroplets emitted by different expiratory activity correspond to four different modes of size distribution, centered on mid-point diameters of respectively D_1 = 0.8, D_2 = 1.8, D_3 = 3.5, and D_4 = 5.5 µm. Their concentrations depend on the expiratory activity as shown in table SM5-1 adapted from Table 1 of Buonanno *et al.* [23]:

Table SM5-1: Concentrations (in cm^{-3}) of the microdroplets size modes during various expiratory activities

	Centered mid-point diameter (µm)			
Expiratory activity	0.80	1.8	3.5	5.5
Voiced counting	0.236	0.068	0.007	0.011
Whispered counting	0.110	0.014	0.004	0.002
Unmodulated vocalization	0.751	0.139	0.139	0.059
Breathing	0.084	0.009	0.003	0.002

It results that equation (SM5-1) can be simplified as:

(SM5-2) $$q_j = VL \times c \times p \times \sum_{i=1}^{i=4} N_{ij} \times V_i$$

where the subscripts i and j refer to the size mode and the expiratory activity respectively.

From equation SM5-2 and Table SM5-1 it is clear that the production rate of quanta can vary widely depending on the expiratory activity but also on the virus strain through VL and c. Note also that the level of activity (which implies a given metabolism) plays an important role on this rate [23]. Therefore, it can change with time for a given infector.

For a given respiratory activity, equation (SM5-2) can be written as:

(SM5-3) $$q = \sum_{i=1}^{i=4} q_i$$

where the subscript j has been omitted.

In the absence of masks for the emitter (infector) and the receiver (susceptible) the dose inhaled by the receiver can be written:

(SM5-4) $$X = \int_0^t n_q^{\infty} \times p \times dt$$

where n_q^∞ is given by equation SM2-6.

When a mask is worn the proportion of particles going through the mask could be strongly dependent of the particle size. Therefore, it could be considered that the quantum production rate is reduced accordingly and that it is possible to define a quantum production rate depending on the mode:

(SM5-5) $$q_i' = \beta_i \times q_i$$

As a conservation equation can be written for each mode, a concentration of quantum for this mode at stationary state will result:

(SM5-6) $$n_{q,i}^\infty = \frac{I \times \beta_i \times q_i}{q_2}$$

If the receiver wears the same kind of masks the inhaled dose of this mode of particles should be:

(SM5-7) $$X_i = \beta_i \times \int_0^t n_{q,i}^\infty \times p \times dt \; = \beta_i^2 \times \int_0^t \frac{I \times q_i}{q_2} \times p \times dt$$

Then the total dose would be:

(SM5-8) $$X = \sum_i X_i$$

For the smallest size, below 1 μm ($i = 1$), the surgical mask can be very inefficient as shown by [25,26] leading to a value of β_i close to 0.5 for the flow through the filtration media.

However due to the importance of the leaks [27], it could be assumed that β_i is also very large even for particles larger than 1 μm (except for the largest ones which behave in a ballistic way and are completely trapped). Then, using equations SM5-7 and SM5-8 with the results of [26,27], it can be shown that wearing the mask reduces the quantum production rate by a factor of three. As the dose of inhaled particles is reduced by the same factor, an overall efficiency in dose reduction of around 90% can be assumed if emitters and receivers wear it, as it has been assumed for schools in the main paper.

SM6- The ICONE index

Based on indoor CO_2 concentrations, the ICONE air stuffiness index [28] has been developed in 2008 by the French Scientific and Technical Center of Building (CSTB) especially for IAQ evaluation in schools. In 2012, the ICONE air stuffiness index has been integrated into the framework for the mandatory monitoring of IAQ in some public buildings in France (IAQ decree n° 2012-14 [29]. The ICONE index takes into account the frequency and intensity of CO_2 levels around the threshold values of 1000 and 1700 ppm during normal occupancy of the classroom by children. The confinement level is then expressed by a score scaled in six levels from 0 to 5. The score 0 corresponds to zero confinement (CO_2 level always below 1000 ppm), this is the most favourable situation. Notes 2 and 3 correspond to low and regular confinement, whereas notes 4 and 5 correspond to very high and extreme confinement, level 5 is the most unfavourable situation (CO_2 concentration always above 1700 ppm during occupancy). In this case, the decree [29] stipulates that additional investigations must be carried out and the local authority (the departmental Prefect) must be informed. Table below summarizes the various situations:

ICONE	Stuffiness level
0	None
1	Weak
2	Moderate
3	High
4	Very high
5	extreme

The icone index can be calculated precisely using the following expression:

$$ICONE = 8.3 \log_{10}(1 + f_1 + 3 f_2)$$

where f_1 and f_2 represent the proportions of CO_2 concentration measurements comprised in between 1000 and 1700 ppm or higher than 1700 ppm respectively. Hence, the ICONE index is zero when all measurements have been found below 1000 ppm ($f_1 = f_2 = 0$) as said earlier whereas it is 5 when all measurements are higher than 1700 ppm ($f_1 = 0$ and $f_2 = 1$).

SM7- The concentration of carbon dioxide as a proxy of the quantum concentration

The exhaled breathing of human beings contains a much higher concentration of carbon dioxide than the normal outdoor air. As a matter of consequence when persons are gathered in a room this leads to a noticeable increase of its concentration as it was recognized by previous authors [30]. Considering the situation depicted in figure SM2-1, a conservation equation for CO_2 can be written in the same way than for particles or quanta:

(SM7-1) $$V \times \frac{dCO_2}{dt} = N_p \times p \times CO_{2,exh} - q_2 \times \{CO_2 - CO_{2,ext}\}$$

with the same notation meaning than in SM2 for V, N_p, p and q_2. CO_2 is the current concentration of CO_2 which can be expressed in ppm (part per million) since air density is assumed constant. $CO_{2,exh}$ and $CO_{2,ext}$ are respectively CO_2 concentration in the air exhaled by a human (close to 40 000 ppm) and outdoor fresh air (around 420 ppm).

The last term of the equation comes from the fact that the fresh outdoor air contains CO_2.

It follows that the carbon dioxide concentration in the room, equal to $CO_2(0)$ at $t = 0$, will evolve following the equation:

(SM7-2) $$CO_2(t) - CO_2(0) = \frac{N_p \times p \times CO_{2,exh}}{q_2} \times \left[1 - exp\left(-\frac{t}{\tau_2}\right)\right]$$

with

(SM7-3) $$\tau_2 = V/q_2$$

Note that most often a "clean" room with a null virus concentration $n_q(0) = 0$ corresponds to $CO_2(0) = CO_{2,ext}$, excepted in un-stationary conditions, for example if ventilation is off during the night and considering a virus lifetime, see end of this SM.

When the quantum (virus) lifetime is very large, τ_1 defined by equation SM2-4 reduces to τ_2. Then, at any time t, it is straightforward to deduce from equations SM2-3, SM2-5 and SM7-2 that:

(SM7-4) $$\frac{n_q(t)}{CO_2(t) - CO_{2,ext}} = \frac{I \times q}{N_p \times p \times CO_{2,exh}}$$

which assumes that at $t = 0$, $CO_2(0) = CO_{2,ext}$ and $n_q(0) = 0$.

Note that it can be shown that the same equation holds for the poorly ventilated case developed in the main paper.

Then using the fact that the dose is:

(SM7-5) $$X = \int_{t_0}^{t_1} n_q \times p \times dt$$

It follows, for a time of exposure $\Delta t = t_1 - t_0$, that:

(SM7-6) $$X = \frac{CO_{2,mean}}{CO_{2,exh}} \times r \times q \times \Delta t$$

with:

(SM7-7) $$CO_{2,mean} = \frac{\int_{t0}^{t1} \Delta CO_2(t) \times dt}{\Delta t} \quad \text{and} \quad \Delta CO_2(t) = CO_2(t) - CO_{2,ext}$$

This equation was first established by Rudnick and Milton [30] in a different way and is valid even for unstationary conditions as long as the virus lifetime $\tau_i \gg V/q_2$.

If the above conditions for τ_i is not fulfilled it is necessary to write a new equation for the dose as a function of time. Still assuming that at $t = 0$, $CO_2(0) = CO_{2,ext}$ and $n_q(0) = 0$, Equation SM7-4 is changed as:

(SM7-8) $$\frac{n_q(t)}{CO_2(t)-CO_{2,ext}} = \frac{I \times q}{N_p \times p \times CO_{2,exh}} \times \frac{q_2}{(q_2 + {}^{V}/_{\tau_i})} \times C(t)$$

with:

(SM7-9) $$C(t) = \frac{\{1-\exp(-{}^{t}/_{\tau_1})\}}{\{1-\exp(-{}^{t}/_{\tau_2})\}}$$

which at stationary state reduces to:

(SM7-10) $$\frac{n_q(t)}{CO_2(t)-CO_{2,ext}} = \frac{I \times q}{N_p \times p \times CO_{2,exh}} \times \frac{q_2}{(q_2 + {}^{V}/_{\tau_i})}$$

and for the dose at stationary state:

(SM7-11) $$X = \frac{CO_{2,mean}}{CO_{2,exh}} \times r \times q \times \Delta t \times \frac{q_2}{(q_2 + {}^{V}/_{\tau_i})}$$

Of course, for transient evolution the dose can be calculated using equation SM7-5 with SM7-8. Now other transient evolutions could be considered with different initial conditions than the choice made above. For example if the ventilation is off overnight the virus lifetime could be such that in the morning ($t = 0$), the conditions $n_q(0) = 0$ holds but with $CO_2(0) > CO_{2,ext}$. In this case $CO_{2,ext}$ should be replaced by $CO_2(0)$ in equations SM7-8 and SM-7-10. These considerations show the importance of the virus lifetime, which is strongly dependent of the room conditions, especially the temperature [31]. Nevertheless, it remains that CO_2 is most often an excellent proxy of the risk, excepted when an air sterilizer at high volume flow rate $q_3 \geq q_2$ is used.

Reference List

[1] W. F. Wells, Airborne Contagion and Air Hygiene. An Ecological Study of Droplet Infections, Harvard University Press, Cambridge, Massachussetts, 1955.

[2] X. M. Bustamante-Marin and L. E. Ostrowski, Cilia and Mucociliary Clearance, Cold Spring Harb. Perspect. Biol., 9 (2017) a028241.

[3] L. E. Kuek and R. J. Lee, First contact: the role of respiratory cilia in host-pathogen interactions in the airways, Am. J. Physiol. Lung Cell Mol. Physiol., 319 (2020) L603-L619.

[4] German Federal Institute for Risk Assessment, Can the new type of coronavirus be transmitted via food and objects?, https://www. bfr. bund. de/cm/349/can-the-new-type-of-coronavirus-be-transmitted-via-food-and-objects. pdf, (2021).

[5] M. Nurminen, T. Nurminen, and C. F. Corvalan, Methodologic issues in epidemiologic risk assessment, Epidemiol., 10 (1999) 585-593.

[6] M. Hoffmann, H. Kleine-Weber, S. Schroeder, N. Krueger, T. Herrler, S. Erichsen, T. S. Schiergens, G. Herrler, N. H. Wu, A. Nitsche, M. A. Mueller, C. Drosten, and S. Poehlmann, SARS-CoV-2 Cell Entry Depends on ACE2 and TMPRSS2 and Is Blocked by a Clinically Proven Protease Inhibitor, Cell, 181 (2020) 271-280.

[7] Y. J. Hou, K. Okuda, C. E. Edwards, D. R. Martinez, T. Asakura, K. H. Dinnon, T. Kato, R. E. Lee, B. L. Yount, T. M. Mascenik, G. Chen, K. N. Olivier, A. Ghio, L. Tse, V, S. R. Leist, L. E. Gralinski, A. Schafer, H. Dang, R. Gilmore, S. Nakano, L. Sun, M. Fulcher, A. Livraghi-Butrico, N. Nicely, I, M. Cameron, C. Cameron, D. J. Kelvin, A. de Silva, D. M. Margolis, A. Markmann, L. Bartelt, R. Zumwalt, F. J. Martinez, S. P. Salvatore, A. Borczuk, P. R. Tata, V. Sontake, A. Kimple, I. Jaspers, W. K. O'Neal, S. H. Randell, R. C. Boucher, and R. S. Baric, SARS-CoV-2 Reverse Genetics Reveals a Variable Infection Gradient in the Respiratory Tract, Cell, 182 (2020) 429-446.

[8] L. Morawska and J. Cao, Airborne Transmission of SARS-CoV-2: The World Should Face the Reality, Environ. Int., 139 (2020) 105730.

[9] J. Wu and P. Zha, Association of COVID-19 Disease Severity with Transmission Routes and Suggested Changes to Community Guidelines, preprint. org, doi:10.20944/preprints202003.0246.v1 (2020).

[10] B. Rockx, T. Kuiken, S. Herfst, T. Bestebroer, M. M. Lamers, B. B. Munnink, D. de Meulder, G. van Amerongen, J. van den Brand, N. M. Okba, D. Schipper, P. van Run, L. Leijten, R. Sikkema, E. Verschoor, B. Verstrepen, W. Bogers, J. Langermans, C. Drosten, M. F. van Vlissingen, R. Fouchier, R. de Swart, M. Koopmans, and B. L. Haagmans, Comparative pathogenesis of COVID-19, MERS, and SARS in a nonhuman primate model, Science, 368 (2020) 1012-1015.

[11] M. Z. Bazant, Video 5-2: Beyond the Well-Mixed Room—Natural Convection, MITOpenCourseWare, (2020) https://ocw.mit.edu/resources/res-10-s95-physics-of-covid-19-transmission-fall-2020/lecture-videos/video-5-2-beyond-the-well-mixed-room2014natural-convection/.

[12] W. Su, B. Yang, A. Melikov, C. Liang, Y. Lu, F. Wang, A. Li, Z. Lin, X. Li, G. Cao, and R. Kosonen, Infection probability under different air distribution patterns, Build. Environ., 207 (2022) 108555.

[13] B. R. Rowe, A. Canosa, J. M. Drouffe, and J. B. A. Mitchell, Simple quantitative assessment of the outdoor versus indoor airborne transmission of viruses and covid-19, Environ. Res., 198 (2021) 111189.

[14] H. Liu, S. He, L. Shen, and J. Hong, Simulation-based study of COVID-19 outbreak associated with air-conditioning in a restaurant, Phys. Fluids, 33 (2021) 023301.

[15] K. S. Kwon, J. I. Park, Y. J. Park, D. M. Jung, K. W. Ryu, and J. H. Lee, Evidence of Long-Distance Droplet Transmission of SARS-CoV-2 by Direct Air Flow in a Restaurant in Korea, J. Kor. Med. Sc., 35 (2020) e415.

[16] J. Lu, J. Gu, K. Li, C. Xu, W. Su, Z. Lai, D. Zhou, C. Yu, B. Xu, and Z. Yang, COVID-19 Outbreak Associated with Air Conditioning in Restaurant, Guangzhou, China, 2020, Emerg. Infect. Dis., 26 (2020) 1628-1631.

[17] T. Toyokawa, T. Shimada, T. Hayamizu, T. Sekizuka, Y. Zukeyama, M. Yasuda, Y. Nakamura, S. Okano, J. Kudaka, T. Kakita, M. Kuroda, and T. Nakasone, Transmission of SARS-CoV-2 during a 2-h domestic flight to Okinawa, Japan, March 2020, Influenza Other Respi. Viruses, 16 (2022) 63-71.

[18] V. Vuorinen, M. Aarnio, M. Alava, V. Alopaeus, N. Atanasova, M. Auvinen, N. Balasubramanian, H. Bordbar, P. Erasto, R. Grande, N. Hayward, A. Hellsten, S. Hostikka, J. Hokkanen, O. Kaario, A. Karvinen, I. Kivisto, M. Korhonen, R. Kosonen, J. Kuusela, S. Lestinen, E. Laurila, H. J. Nieminen, P. Peltonen, J. Pokki, A. Puisto, P. Raback, H. Salmenjoki, T. Sironen, and M. OOsterberg, Modelling aerosol transport and virus exposure with numerical simulations in relation to SARS-CoV-2 transmission by inhalation indoors, Saf. Sc., 130 (2020) 104866.

[19] R. C. Flagan and J. H. Seinfeld, Fundamentals of Air Pollution Engineering, Prentice Hall Inc., Englewood Cliffs, New Jersey (USA) 1988.

[20] W. Chen, N. Zhang, J. Wei, H. L. Yen, and Y. Li, Short-range airborne route dominates exposure of respiratory infection during close contact, Build. Environ., 176 (2020) 106859.

[21] G. Cortellessa, L. Stabile, F. Arpino, D. E. Faleiros, W. V. Bos, L. Morawska, and G. Buonanno, Close proximity risk assessment for SARS-CoV-2 infection, Sc. Tot. Environ., 794 (2021) 148749.

[22] L. Gammaitoni and M. C. Nucci, Using a mathematical model to evaluate the efficacy of TB control measures, Emerg. Infect. Dis., 3 (1997) 335-342.

[23] G. Buonanno, L. Stabile, and L. Morawska, Estimation of airborne viral emission: Quanta emission rate of SARS-CoV-2 for infection risk assessment, Environ. Int., 141 (2020) 105794.

[24] L. Morawska, G. R. Johnson, Z. D. Ristovski, M. Hargreaves, K. Mengersen, S. Corbett, C. Y. H. Chao, Y. Li, and D. Katoshevski, Size distribution and sites of origin of droplets expelled from the human respiratory tract during expiratory activities, Aerosol Sc., 40 (2009) 256-269.

[25] C. C. Chen and K. Willeke, Aerosol Penetration Through Surgical Masks, Am. J. Infect. Cont., 20 (1992) 177-184.

[26] A. Weber, K. Willeke, R. Marchioni, T. Myojo, R. Mckay, J. Donnelly, and F. Liebhaber, Aerosol Penetration and Leakage Characteristics of Masks Used in the Health-Care Industry, Am. J. Infect. Cont., 21 (1993) 167-173.

[27] S. Rengasamy, B. C. Eimer, and J. Szalajda, A Quantitative Assessment of the Total Inward Leakage of NaCl Aerosol Representing Submicron-Size Bioaerosol Through N95 Filtering Facepiece Respirators and Surgical Masks, J. Occup. Environ. Hyg., 11 (2014) 388-396.

[28] Ribéron, J., Ramalho, O., Mandin, C., and Cochet, V. Guide d'application pour la surveillance du confinement de l'air dans les établissements d'enseignement, d'accueil de la petite enfance et d'accueil de loisirs. DESE/Santé N°2012-086R, 1. 2012. CSTB, Département Energie Santé Environnement, Division Santé.

[29] JORF, Décret n° 2012-14 du 5 janvier 2012 relatif à l'évaluation des moyens d'aération et à la mesure des polluants effectuées au titre de la surveillance de la qualité de l'air intérieur de certains établissements recevant du public, https://www. legifrance. gouv. fr/loda/id/JORFTEXT000025105291/2021-12-27/, (2012) txt17.

[30] S. N. Rudnick and D. K. Milton, Risk of indoor airborne infection transmission estimated from carbon dioxide concentration, Indoor Air, 13 (2003) 237-245.

[31] T. F. Yap, Z. Liu, R. A. Shveda, and D. J. Preston, A predictive model of the temperature-dependent inactivation of coronaviruses, Appl. Phys. Lett., 117 (2020) 060601.